

Work of fracture of high impact polystyrene (HIPS) film under plane stress conditions

S. HASHEMI

London Metropolitan University, London Metropolitan Polymer Centre, London N7 8DB, UK
E-mail: s.hashemi@londonmet.ac.uk

Essential work of fracture methodology was used to determine plane-stress ductile fracture toughness of high impact polystyrene film of thickness 0.26 mm. Results obtained indicated that specific essential work of fracture, w_e , is independent of loading rate, and for certain specimen sizes, independent of both gauge length and width of the specimen. On the other hand, w_e was found to be affected by the temperature, molecular anisotropy and the geometry of the test specimens. Reasonable estimate of w_e was obtained via crack opening displacement value. © 2003 Kluwer Academic Publishers

1. Introduction

It has been shown that for materials that show significant crack tip plasticity, techniques such as J-integral and the Essential Work of Fracture (EWF) must be used to quantify fracture toughness. Although the J-integral approach has been used traditionally for this purpose, the EWF method has gained popularity due to its experimental simplicity as the method avoids the measurement of the current crack advance as well as the detection of cracking initiation. EWF methodology offers an attractive means for separating the energy spent in the fracture process zone from the work spent in the plastic deformation zone surrounding the fracture process zone. According to EWF which was first developed by Broberg [1] and further developed by Cotterell and Reddel [2], a linear dependence exists between the specific total work of fracture and ligament length, giving a positive intercept at zero ligament length. The positive intercept is termed the specific essential work of fracture, w_e , which is an indicator of the crack propagation resistance. Recent studies have shown that EWF approach can be used successfully to characterize ductile fracture of polymeric materials under plane-stress conditions [e.g., 3–21].

The purpose of this paper is to study in detail the fracture behaviour of high impact polystyrene sheet by analysing the EWF test results obtained by varying the size and the geometry of the specimen, the test temperature and loading rate. The effect of molecular anisotropy on EWF parameters is also examined.

2. Essential work of fracture methodology and restrictions

Broberg [1] stated that when ultimate failure of the pre-notched specimens is preceded by extensive yielding and slow crack growth, a toughness parameter called “Specific Essential Work of Fracture, w_e ” can be evaluated, representing the work required for crack propagation under plane-stress conditions. In this analysis,

fracture is modelled as consisting of two zones: the inner fracture process zone (IFPZ) and the outer plastic deformation zone (OPDZ). Fig. 1 shows schematic representation of the two zones in a single edge and a double-edged notched tension specimens. The IFPZ is where fracture actually takes place and OPDZ is where various types of plastic deformation such as shear yielding and microvoiding may be operating. Based on this concept, the total work of fracture, W_f (the total area under a P - δ curve) may be partitioned into two components: the Essential Work of Fracture (W_e) and Non-Essential Work of Fracture (W_p). Thus the following relation can be written:

$$W_f = W_e + W_p \quad (1)$$

The term W_e is essentially a surface energy term whose value is proportional to the ligament area (LB), i.e.,

$$W_e = w_e BL \quad (2)$$

The term w_e is called the “Specific Essential Work of Fracture,” considered to be a material constant for a given thickness.

The term W_p is a volume-related energy term whose value is proportional to the volume of the yielded zone. Thus

$$W_p = w_p \beta BL^2 \quad (3)$$

The term w_p is called the “Specific Non-Essential Work of Fracture” and β is the plastic zone shape factor. Thus inserting Equations 2 and 3 into Equation 1 and rearranging gives;

$$w_f = \frac{W_f}{LB} = w_e + \beta w_p L \quad (4)$$

where w_f is termed the “Specific Total Work of Fracture.”

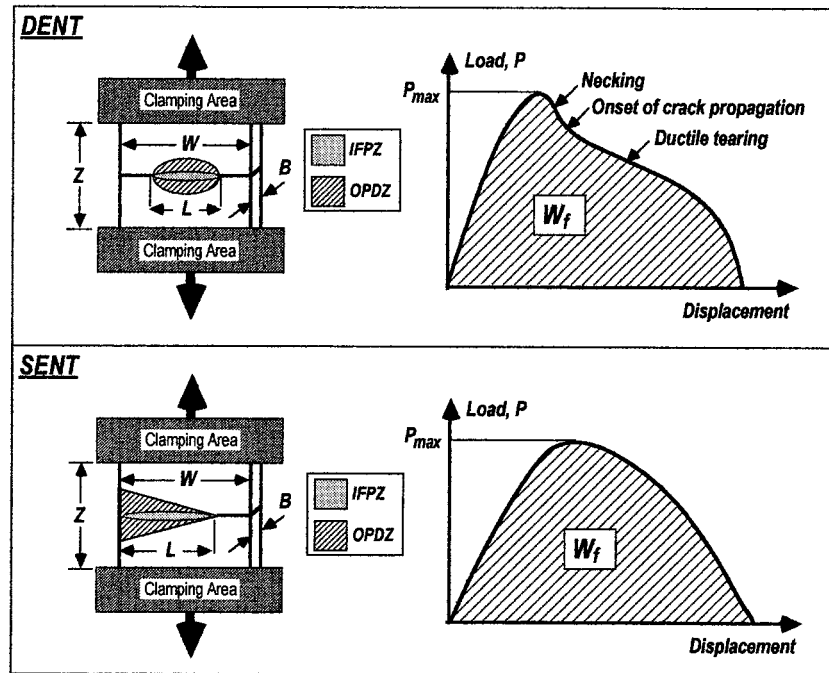


Figure 1 SENT and DENT type specimen geometry and their load-displacement digramms.

According to Equation 4, w_e can be obtained by carrying out a linear regression on the values of the specific work of fracture w_f measured for a range of specimens with different ligament lengths. The intercept with the w_f -axis at $L = 0$ and the slope would give respectively the values of w_e and βw_p . However, for such linearity to apply, the regression must be performed on ligament lengths large enough as to warrant that all the specimens present globally the same stress state across the ligament region. Typically, the ligament length must be equal to about 3–5 times the specimen thickness. In the meantime, the ligament length must be small enough as to avoid the disconnection of the plastic zones (the ligament length must be fully yielded— this condition is usually verified when the ligament length is smaller than twice the radius of the plastic zone at the crack tip) and to avoid the spreading of the plastic zone to the boundaries of the specimen (this condition is usually verified when the ligament length is smaller than one third of the specimen width). To satisfy these conditions, the ESIS protocol for EWF [22] recommends the following restrictions to be placed upon the length of the ligament region:

$$L_{\min} = 3B - 5B$$

$$L_{\max} = \min\left(\frac{W}{3}, 2R_p\right) \quad (5)$$

where B is the specimen thickness, W is the specimen width and R_p is the radius of the plastic zone whose value can be estimated from the following equation

$$R_p = \frac{1}{2\pi} \frac{E w_e}{\sigma_y^2} \quad (6)$$

E and σ_y are respectively, the elastic modulus and tensile yield stress of the material.

3. Experimental

High impact polystyrene extruded sheet 0.26 mm thick, 500 mm wide and several meters in length was supplied by Witt plastics, inc (grade W-1301). The sheet was 0.26 mm thick, 500 mm wide and several meters in length. The material used has melt flow index of 3 g/10 min, density 1040 kg/m³ and containing 90% graft copolymer of styrene on a dienic unsaturated-rubber. The EWF tests were performed on rectangular coupons cut from the sheet such that the length of the coupons was either normal or parallel to the extrusion direction. The initial notches were subsequently inserted perpendicular to the long edge of the coupons using a fresh razor blade to produce series of Double Edge Notched Tension (DENT) and Single Edge Notched Tension (SENT) specimens as shown in Fig. 1. At least twenty specimens with ligament lengths, L , varying between 4 and 16 mm were prepared for determining a w_e -value. The ligament length was measured before the test using a travelling binocular lens microscope. Each specimen was then tested to complete failure in an Instron testing machine. The specimen dimensions and test conditions are given in the relevant sections. The load-displacement (P - δ) curve for each specimen was recorded using computer data logger and the absorbed energy (W_f) calculated by integration of the area under the curve.

4. Results and discussions

4.1. Effect of specimen type on EWF parameters

SENT and DENT type specimens with $W = 35$ mm, $Z = 70$ mm and with initial notches in the extrusion direction were tested at 25°C at crosshead displacement rate value of 5 mm/min. Fig. 1 shows schematic

representation of the type of load-displacement (P - δ) curves obtained for each specimen type.

As depicted in Fig. 1, whilst P - δ curves obtained for the two specimen types differ in shape, both are indicative of a ductile failure. Most importantly, it was observed that for each specimen type, curves obtained were similar to one another for different ligament lengths, which is the essential pre-requisite for EWF testing. The total area under the curve, W_f , the maximum load, P_{\max} , and the elongation at break, e_f , all increased with increasing L .

From the visual detection of the specimens during the test, the following observations were made;

- Failure of the DENT specimens occurred after crack tip yielding which appeared as stress-whitened region. Full yielding of the ligament region in DENT specimens occurred at maximum load (P_{\max}) and before crack propagation started. The subsequent necking of the fully yielded ligament region in DENT specimens gave rise to a prominent load drop after maximum load (see Fig. 1). At this point, crack began propagating by ductile tearing of the necked-down region. Clearly, the behaviour noted for DENT specimens validates the use of the EWF for the treatment of the data.
- Failure of the SENT specimens occurred after crack tip yielding which appeared as stress-whitened region. The full yielding of the ligament region in this specimen type occurred after maximum load was reached and the propagation of the crack began before ligament length was yielded fully. Strictly speaking, the behaviour noted for SENT specimens invalidates the use of the EWF for the treatment of the data.

Values of the specific total work of fracture, w_f , for both DENT and SENT specimens are plotted against ligament length in Fig. 2a. It is seen that SENT geometry fractures at a higher w_f value compared to DENT of the same ligament length. However, whilst variation is linear over the entire ligament length range for DENT specimens, it tends to deviate from this linear trend for SENT specimens as ligament length exceeds 12 mm ($\approx W/3$). The most likely scenario is that the plastic zone size in SENT specimens no longer increases in proportion to the ligament length either because $L_{\max} > W/3$ (i.e., edge effects) or that $L_{\max} > 2R_p$, the latter will be revisited later.

It worth noting that since the smallest ligament length used in this study is $20B$, it is reasonable to assume that the state of stress in the ligament regions is that of pure plane-stress. The plane-stress criterion was nonetheless checked against Hill's analysis [23] by plotting the values of net-section stress at maximum load, σ_n ($=P_{\max}/LB$) against ligament length. The results are shown in Fig. 2b where it can be seen that whilst DENT specimens exhibit higher values of σ_n compared to SENT specimens due to notch constraint effect, a similar dependence on L is obtained for both specimen types. Evidently, for ligament lengths smaller than 7 mm or thereabouts, σ_n rises with decreasing L ,

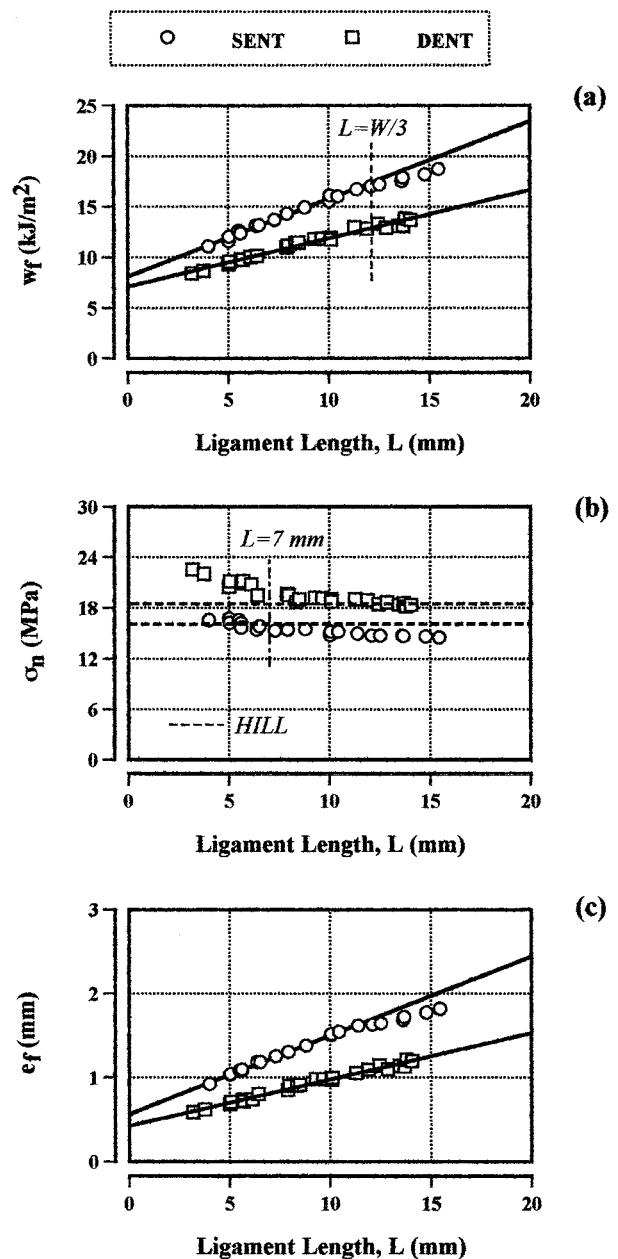


Figure 2 (a) Specific work of fracture versus ligament length for SENT and DENT type specimens. (b) Net-section stress versus ligament length for SENT and DENT type specimens. (c) Extension to break versus ligament length for SENT and DENT type specimens.

whereas for long ligament lengths $\sigma_{ns} \approx \sigma_y$ for SENT and $\sigma_{ns} \approx 1.15\sigma_y$ for DENT specimens, as predicted by Hill (σ_{ns} represents the steady state value of σ_n). Assuming that the stress state transition in HIPS does indeed occur at $L = 7$ mm, then $L_{\min} = 27B$ and not the recommended value of $3B$ - $5B$. However, as this transition is not reflected in w_f versus L plots, we can only suggest that perhaps the constraint effects were not significantly large enough to affect the w_f values.

Following Equation 4, we obtain from the regression lines in Fig. 2a that

$$w_e = 7.10 \text{ kJ m}^{-2}, \quad \beta w_p = 0.48 \text{ MJ m}^{-3} \quad (\text{DENT})$$

$$w_e = 8.09 \text{ kJ m}^{-2}, \quad \beta w_p = 0.77 \text{ MJ m}^{-3} \quad (\text{SENT})$$

Results show that EWF parameters obtained via SENT specimens are greater than those obtained via DENT specimens. However, whilst the difference in w_e is no more than 15%, βw_p for SENT is approximately 1.5 times greater. This is possibly due to the difference in the plastic zone shape factor, β , of the two specimen types.

Having determined w_e , it is worth considering the relevance of the pre-requisite $L_{\max} < 2R_p$. Substituting for $E = 1.78$ GPa and for $\sigma_y = 16$ MPa into Equation 6 gave $2R_p$ values of 16 and 18 mm for DENT and SENT type specimens respectively, indicating that $W/3 < 2R_p$ for both specimen types. The onset of nonlinearity in w_f versus L plot for SENT specimens at $L \approx 12$ mm could therefore be due to edge effects and if so, the upper threshold value $L_{\max} = W/3$ appears more suited to SENT type specimen than DENT type. It is worth stating that whilst the pre-requisite $L_{\max} < \min(W/3, 2R_p)$ provides a safe upper bound working limit for the ligament length, it is often found to be too stringent [e.g., 8, 10, 12, 14–17, 20, 21].

It has been shown in several studies [e.g., 4, 10, 12, 14, 17, 19–21] that the parameter w_e may be estimated reasonably well via crack opening displacement (COD) of the advancing crack tip using a simple relationship of the form

$$w_e = M\sigma_y \text{ COD} \quad (7)$$

where M is plastic constraint factor whose value for SENT is unity and for DENT is 1.15 (product $M\sigma_y$ represents the state-steady state value of net-section stress, σ_{ns}).

To obtain COD, the extension to break values, e_f , were plotted against ligament length. As shown in Fig. 2c, a linear dependence exists between the two parameters, i.e.,

$$e_f = e_o + e_p L \quad (8)$$

The intercept value e_o has been identified as the COD of the advancing crack tip [e.g., 4, 10, 12, 14, 17, 19–21] and the slope, e_p , as the plastic contribution to extension. A linear regression on the values of e_f versus L in Fig. 2c for each specimen type gave the following relationships;

$$e_f = 0.43 + 0.055 L \quad (\text{DENT})$$

$$e_f = 0.56 + 0.094 L \quad (\text{SENT})$$

It can be seen that the e_o and e_p are both affected by the geometry of the test specimen. Using Equation 7, we obtain w_e values of 7.90 kJ m^{-2} and 8.96 kJ m^{-2} for DENT and SENT type specimens respectively; both values being greater than the directly measured values by approximately 12%. However, considering that e_f measurements are approximate since they are obtained from elongation for the entire specimen, and not by using clip-gauges across the outer plastic zone, estimated values of w_e seem reasonable.

4.2. Specimen size effect on EWF parameters

Influence of the specimen size on EWF parameters was studied using DENT type specimens with initial notches in the extrusion direction. Two sets of specimens were prepared for this study. In one set, specimens had a constant W of 35 mm with Z varying between 15 and 90 mm and in the other set, specimens had a constant Z of 70 mm with W varying between 15 and 45 mm. All the specimens were fractured at 25°C at a constant displacement rate of 5 mm/min. The load-displacement curves produced showed no significant change in shape with varying specimen size. Most importantly, curves obtained for different ligament lengths were geometrically similar to one another for a given specimen size.

Fig. 3a and b shows the plots of w_f versus L for different values of Z and W . Results show a linear dependence between w_f and L over the entire ligament length range for all specimen sizes under

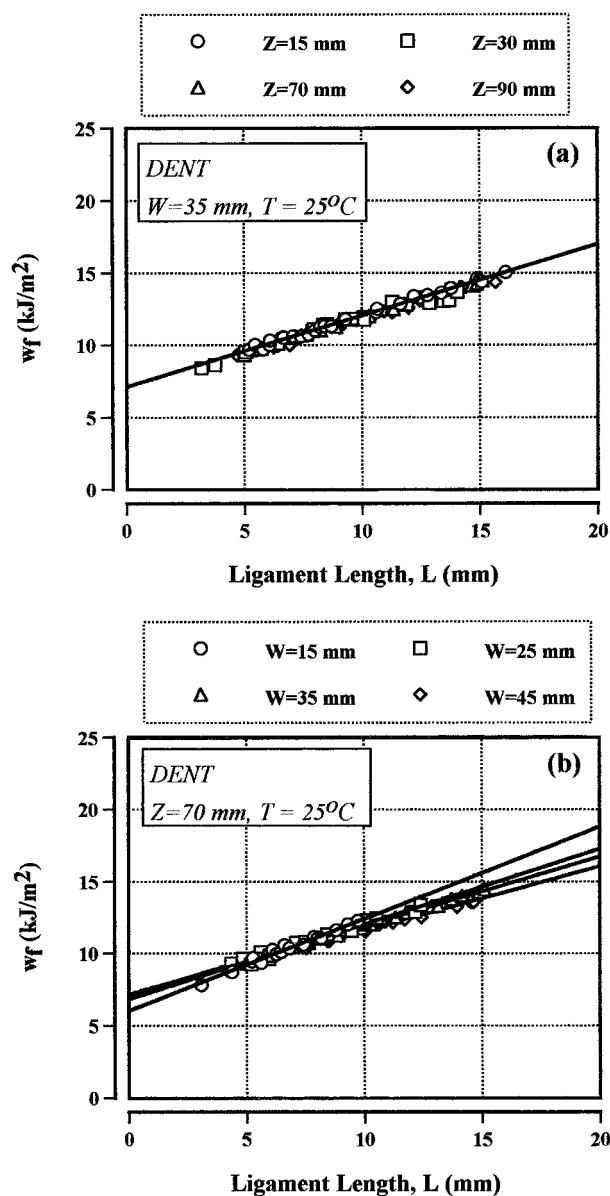


Figure 3 (a) Specific work of fracture versus ligament length for different specimen gauge lengths. (b) Specific work of fracture versus ligament length for different specimen widths.

TABLE I Gauge length effect on EWF parameters ($W = 35$ mm, $v = 5$ mm/min, $T = 25^\circ\text{C}$)

	$Z = 15$ mm	$Z = 30$ mm	$Z = 70$ mm	$Z = 90$ mm
w_e (kJ/m ²)	7.13	7.10	7.12	7.09
βw_p (MJ/m ³)	0.49	0.48	0.48	0.47
e_o (mm)	0.44	0.43	0.44	0.42
$^a w_e$ (kJ/m ²)	8.10	7.92	8.10	7.73

^aEstimated via Equation 7.

TABLE II Specimen width effect on EWF parameters ($Z = 70$ mm, $v = 5$ mm/min, $T = 25^\circ\text{C}$)

	$W = 15$ mm	$W = 25$ mm	$W = 35$ mm	$W = 45$ mm
w_e (kJ/m ²)	6.03	6.90	7.12	7.15
βw_p (MJ/m ³)	0.64	0.52	0.48	0.44
e_o (mm)	0.37	0.41	0.44	0.45
$^a w_e$ (kJ/m ²)	6.81	7.55	8.10	8.28

^aEstimated via Equation 7.

consideration, indicating that the plastic zone size in these specimens increased in proportion to the ligament length. Linear extrapolation of the data for each specimen size gave values of w_e and βw_p listed in Tables I, II.

Table I shows that varying Z had no significant influence upon values of w_e and βw_p as regression lines tends to merge to a single line (see Fig. 3a). On the other hand, it can be seen from Table II that varying W has affected both parameters, with w_e increasing and βw_p decreasing with increasing width. However, whilst βw_p term decreases progressively, w_e achieves a steady state value of 7.13 kJ m⁻² at large widths. It seems that for HIPS there is a minimum threshold specimen width (≈ 25 mm) below which w_e shows a dependence on specimen width.

As for the effect of specimen size on σ_n , it can be seen from plots in Fig. 4a and b that σ_n is not affected by the size of the test specimen, at least within the range for which w_e is specimen size independent. Variation of σ_n with L shows that $\sigma_n \approx 1.15\sigma_y$ at large ligament lengths but increases with decreasing L at short ligament lengths with a transition point at $L \approx 7$ mm.

The effect of varying Z and W on extension to break versus ligament length plot is shown in Fig. 5a and b where it can be seen that extension to break increases linearly with L over the entire range for all specimen sizes under consideration. As summarised in Tables I and II, e_o shows no significant variation with respect to Z but with respect to specimen width, it shows a dependence which is similar to that observed for w_e . As shown in Tables I and II e_o provides a reasonable estimate of w_e .

4.3. Temperature effect on EWF parameters

The effect of temperature on EWF parameters was studied using DENT type specimens with $W = 35$ mm and $Z = 30$ mm and their length normal to the extrusion direction. The tests were performed be-

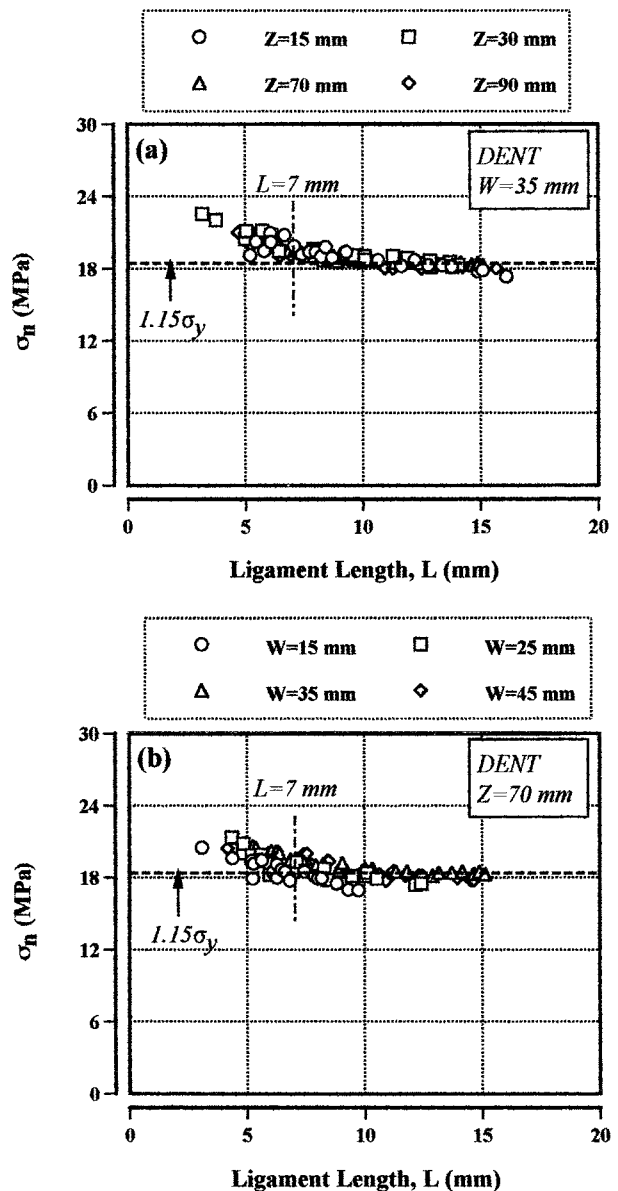


Figure 4 (a) Net-section stress versus ligament length for different specimen gauge lengths. (b) Net-section stress versus ligament length for different specimen widths.

tween 25°C and 80°C at displacement rate value of 5 mm/min. Within this temperature range, failure of the specimens was stable and ductile. The crack propagation was observed to occur after ligament yielding at all test temperatures. The load-displacement curves indicated that as temperature is raised, the load level decreases but the total deformation increases. The geometrical similarity between P - δ curves was maintained over the entire temperature range under consideration.

Fig. 6a shows the effect of varying temperature on w_f versus L plot. The dependence of w_f on ligament length is linear at all test temperatures and over the entire ligament length range under consideration. It can be seen that an increase in temperature produces a progressive drop in w_f values. The results of the EWF fracture parameters as a function of temperature are summarised in Table III and their trend with respect to temperature is illustrated in Fig. 6b. It is seen that w_e and βw_p for HIPS decrease progressively with increasing temperature. It

TABLE III Temperature effect on EWF parameters ($W = 35$ mm, $Z = 30$ mm, $v = 5$ mm/min)

	$T = 25^\circ\text{C}$	$T = 40^\circ\text{C}$	$T = 60^\circ\text{C}$	$T = 80^\circ\text{C}$
w_e (kJ/m ²)	7.10	6.87	6.09	5.02
βw_p (MJ/m ³)	0.48	0.44	0.36	0.21
e_o (mm)	0.43	0.50	0.52	0.57
σ_y (MPa)	16.01	12.93	10.60	9.00
E (GPa)	1.78	1.62	1.49	1.35
$2R_p$ (mm)	15.71	20.88	25.71	26.63
^a w_e (kJ/m ²)	7.92	7.43	6.34	5.90

^aEstimated via Equation 7.

is worth stating that EWF measurements were not possible at 100°C , as DENT specimens deformed rather than fracturing.

The plane-stress criterion at each temperature was checked against Hill's analysis. The results are shown in Fig. 7a and they agree well with the predicted value

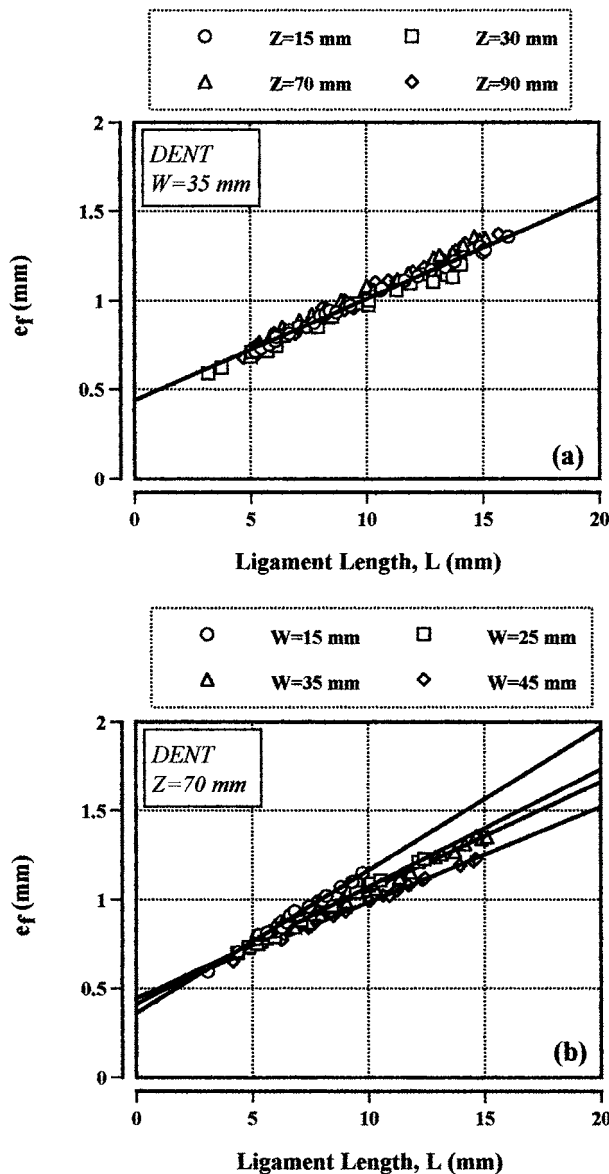


Figure 5 (a) Extension at break versus ligament length for different specimen gauge lengths. (b) Extension at break versus ligament length for different specimen widths.

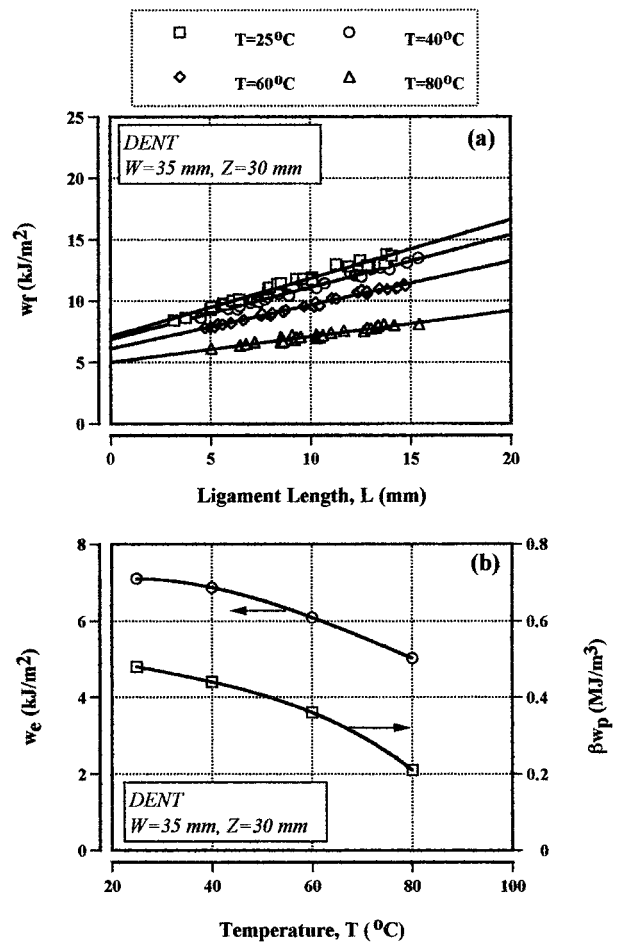


Figure 6 (a) Specific work of fracture versus ligament length at various temperatures. (b) Specific essential and non-essential work of fracture versus temperature.

of $1.15\sigma_y$ (values of tensile yield stress as a function of temperature can be found in Table III). According to Fig. 7a, transition in stress state occurs at $L \approx 7$ mm for all test temperatures.

The linearity between extension to break and ligament length is also maintained over the entire temperature range under consideration as illustrated in Fig. 7b. Table III shows that the value of e_o increases with increasing temperature.

The dependence of w_e on temperature can be explained in terms of the variation of the terms included in Equation 7. The observed decrease in w_e with temperature implies that decrease in $M\sigma_y$ outweighs the increase in e_o , as temperature rises. As demonstrated in Table III, values of w_e estimated using Equation 7 are in good agreement with the extrapolated values obtained from Fig. 7. As for the effect of temperature on βw_p term, we can only assume that the trend obtained is resulted from a competition between the shape factor β and the plastic energy density w_p .

Finally, it can be seen from Table III, that calculated values of $2R_p$ are greater than $W/3$. In the absence of any nonlinearity in w_f versus L plots at $L = W/3$, we conclude once again that the pre-requisite $L < W/3$ is too restrictive.

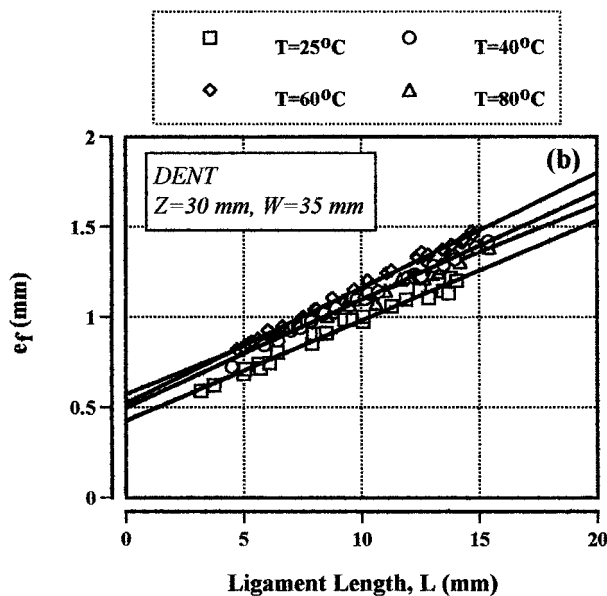
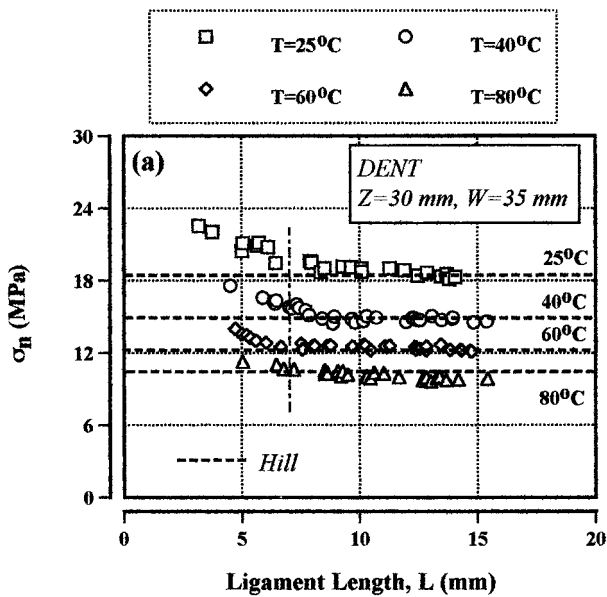


Figure 7 (a) Net-section stress versus ligament length at various temperatures. (b) Extension to break versus ligament length at various temperatures.

4.4. Loading rate effect on EWF parameters
DENT specimens with $Z = 30$ mm, $W = 35$ mm and with their length perpendicular to the extrusion direction were used for this study. These specimens were fractured at 25°C at loading rate values ranging from 1 to 50 mm/min. Within this range, fracture was stable and ductile producing load-displacement curves similar to that depicted in Fig. 1.

Fig. 8 shows the plot of w_f versus L at different loading rates. The best linear regression lines gave the following results;

$$w_f = 7.05 + 0.36 L \quad (v = 1 \text{ mm/min})$$

$$w_f = 7.10 + 0.48 L \quad (v = 5 \text{ mm/min})$$

$$w_f = 7.12 + 0.66 L \quad (v = 50 \text{ mm/min})$$

Results show that w_e is rate insensitive, whereas βw_p rises progressively with increasing rate.

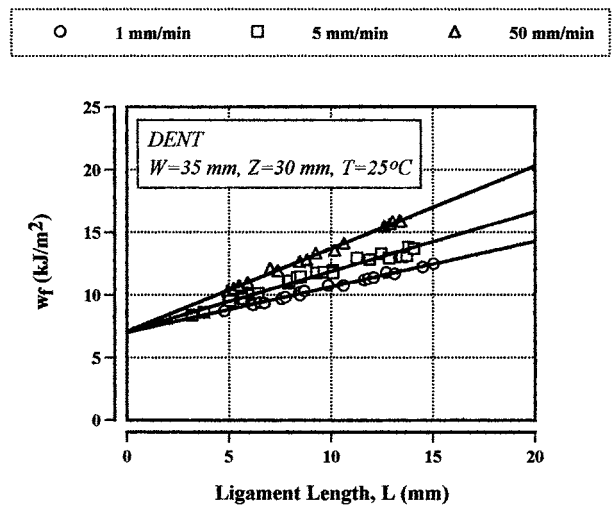


Figure 8 Specific work of fracture versus ligament length at different loading rates.

4.5. Effect of molecular anisotropy on EWF parameters

The results obtained thus far relate to specimens whose lengths were normal to the extrusion direction of the sheet (TD specimens). To investigate the effect of anisotropy on EWF parameters, DENT specimens with $W = 35$ mm were prepared such that length of the specimens was parallel to the extrusion direction (FD specimens), i.e., the initial cracks were normal to extrusion direction. These specimens were fractured between 25°C and 80°C at a constant crosshead displacement of 5 mm/min with $Z = 30$ mm. Within this temperature range, failure of the FD specimens like TD specimens was stable and ductile. The overall shape of the FD load-displacement curves was similar to TD specimens. However, for the same ligament length and at the same test temperature, FD specimens exhibited higher extension to break and load level values than TD specimens. For this reason, w_f for FD specimens was significantly higher, as w_f versus L plots in Fig. 9 demonstrates. Plots of extension to break e_f and net-section stress σ_n versus ligament length maintained their general trends, i.e., e_f increased linearly and σ_n decreased with increasing L . Results obtained from FD specimens are summarised in Table IV where it can be seen that values of w_e , βw_p and e_o obtained from FD specimens are greater than TD specimens, but having a similar dependence on temperature as TD specimens.

TABLE IV Anisotropy effect on EWF parameters ($W = 35$ mm, $Z = 30$ mm, $v = 5$ mm/min)

		$T = 25^\circ\text{C}$	$T = 40^\circ\text{C}$	$T = 60^\circ\text{C}$	$T = 80^\circ\text{C}$
w_e (kJ/m ²)	TD	7.10	6.87	6.09	5.02
	FD	8.88	8.27	7.72	5.86
βw_p (MJ/m ³)		0.48	0.43	0.36	0.22
		0.97	0.81	0.53	0.40
e_o (mm)		0.43	0.50	0.52	0.58
		0.50	0.57	0.60	0.65
$^a w_e$ (kJ/m ²)	FD	9.78	9.18	7.80	6.51

^aEstimated via Equation 7.

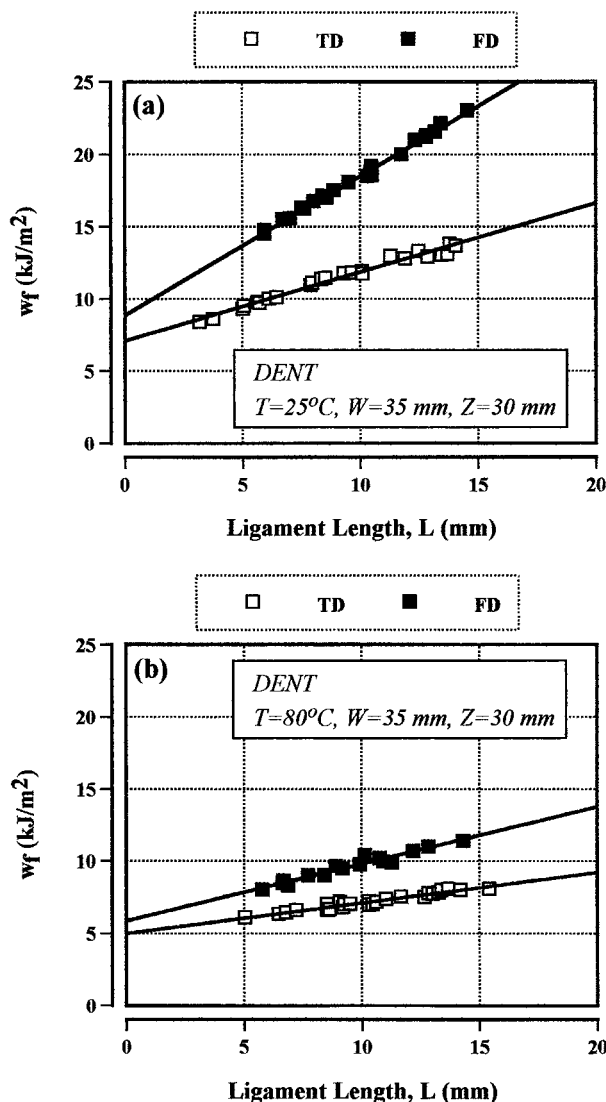


Figure 9 (a) Specific work of fracture versus ligament length for TD and FD specimens at 25°C. (b) Specific work of fracture versus ligament length for TD and FD specimens at 80°C.

5. Conclusions

EWF technique was used to characterise fracture toughness of high impact polystyrene (HIPS) film under plane-stress conditions. Results obtained led to the following conclusions;

1. Specific essential work of fracture (w_e) and specific non-essential work of fracture (βw_p) for SENT type specimens were greater than for DENT type.

2. w_e and βw_p were independent of specimen gauge length but were specimen width dependent, with w_e increasing and βw_p decreasing with increasing width.

3. w_e and βw_p both decreased whilst COD of the advancing crack tip increased with increasing temperature.

4. w_e was rate insensitive whereas βw_p increased with increasing rate.

5. Values of w_e and βw_p were consistently higher when the initial crack propagated normal to the extrusion direction as oppose to propagating along the extrusion direction.

References

1. K. B. BROBERG, *Int. J. Fract.* **4** (1968) 11.
2. B. COTTERELL and J. K. REDDEL, *ibid.* **13** (1977) 267.
3. Y. W. MAI, B. COTTERELL, R. HORLYCK and G. VIGNA, *Polym. Eng. Sci.* **27** (1987) 804.
4. S. HASHEMI, *Plast. Rub. Comp. Proc. Appl.* **20** (1993) 229.
5. J. WU, Y. W. MAI and B. COTTERELL, *J. Mater. Sci.* **28** (1993) 3373.
6. W. Y. F. CHAN and J. G. WILLIAMS, *Polymer.* **35** (1994) 1666.
7. J. WU and Y. W. MAI, *Polym. Eng. Sci.* **36** (1996) 2275.
8. J. KARGER-KOCSIS and T. CZIGANY, *Polymer.* **37** (1996) 2433.
9. J. KARGER-KOCSIS, T. CZIGANY and E. J. MOSKALA, *ibid.* **38** (1997) 4587.
10. S. HASHEMI, *J. Mater. Sci.* **32** (1997) 1573.
11. J. KARGER-KOCSIS, T. CZIGANY and E. J. MOSKALA, *Polymer.* **39** (1998) 3939.
12. A. ARKHIREYEVA, S. HASHEMI and M. O'BRIEN, *J. Mater. Sci.* **34** (1999) 5961.
13. J. J. CASELLAS, P. M. FRONTINI and J. M. CARELLA, *J. Appl. Polym. Sci.* **74** (1999) 781.
14. S. HASHEMI and J. G. WILLIAMS, *Plast. Rubb. Compos.* **29** (2000) 294.
15. S. HASHEMI, *Polym. Eng. Sci.* **40** (2000) 132.
16. *Idem.*, *ibid.* **40** (2000) 798.
17. *Idem.*, *ibid.* **40** (2000) 1435.
18. E. C. Y. CHING, R. K. Y. LI and Y. W. MAI, *ibid.* **40** (2000) 310.
19. D. E. MOUZAKIS, J. KARGER-KOCSIS and E. J. MOSKALA, *J. Mater. Sci., Lett.* **19** (2000) 1615.
20. A. ARKHIREYEVA and S. HASHEMI, *Plast. Rubb. Compos.* **30** (2001) 125.
21. *Idem.*, *J. Mater. Sci.* **37** (2002) 3675.
22. Test Protocol for Essential Work of Fracture, Version 5, ESIS TC-4 Group, Les Diablerets, 1998.
23. R. H. HILL, *J. Mech. Phys. Solids* **1** (1952) 19.

Received 8 October 2002
and accepted 18 April 2003